AIMS Bioengineering, 3(3): 277-288.
DOI: 10.3934/bioeng.2016.3.277
Received: 09 June 2016
Accepted: 15 July 2016
Published: 17 July 2016

http://www.aimspress.com/journal/Bioengineering

Research article

Assembly of a functional 3D primary cardiac construct using magnetic levitation

Matthew Hogan [1], Glauco Souza [2], Ravi Birla [1,*]

[1] Department of Biomedical Engineering, University of Houston, Houston, TX, USA
[2] Nano3D Biosciences, Houston, TX, USA

*** Correspondence:** Email: rkbirla@uh.edu; Tel: +1-832-842-8813.

Abstract: Easily assembled organotypic co-cultures have long been sought in medical research. *In vitro* tissue constructs with faithful representation of *in vivo* tissue characteristics are highly desirable for screening and characteristic assessment of a variety of tissue types. Cardiac tissue analogs are particularly sought after due to the phenotypic degradation and difficulty of culture of primary cardiac myocytes. This study utilized magnetic nanoparticles and primary cardiac myocytes in order to levitate and culture multicellular cardiac aggregates (MCAs). Cells were isolated from 2 day old Sprague Dawley rat hearts and subsequently two groups were incubated with either C_1: 33 μL nanoshell/million cells or C_2: 50 μL nanoshell/million cells. Varying numbers of cells for each concentration were cultured in a magnetic field in a 24 well plate and observed over a period of 12 days. Constructs generally formed spherical structures. Masson's trichrome staining of a construct shows the presence of extracellular matrix protein, indicating the presence of functional fibroblasts. Many constructs exhibited noticeable contraction after 4 days of culture and continued contracting noticeably past day 9 of culture. Noticeable contractility indicates the presence of functional primary cardiac myocytes in culture. Phenotypic conservation of cardiac cells was ascertained using IHC staining by α-actinin and collagen. CD31 and fibrinogen were probed in order to assess localization of fibroblasts and endothelial cells. The study verifies a protocol for the use of magnetic levitation in order to rapidly assemble 3D cardiac like tissue with phenotypic and functional stability.

Keywords: cardiac; tissue engineering; heart muscle; levitation

1. Introduction

Three-dimensional (3D) cell culture systems have been a critical area of biomedical research for decades. In recent years, the importance of a cost-effective, serviceable 3D culture system has become increasingly apparent (1-8). While two-dimensional (2D) cell culture experiments have been the primary method of discovery since the inception of cell research, there are innate limits to such methods. The gaps in complexity and fidelity between 2D cultures and native tissues limit potential of research in flat culture environments. De-differentiation, lack of multi-dimensional cell-cell connectivity and inter-dimensional simplicity all contribute to the fundamental shortfalls of traditional culture models.

Organotypic culture systems, thus, have been a central area of concern in biomedical research for decades. Development of efficacious high throughput drug screening (HTS) on tissue-mimetic models represents a holy grail in the field. Organotypic culture systems must meet several criteria in order to become widely used. One major concern is cost. Excessive equipment, reagents and/or biological materials are limiting factors in research. Streamlining materials and simplifying the model can reduce such costs and make an organotypic culture system more palatable for product development. Furthermore, while complex models can work in the laboratory, set-up time, training, labor and additional variables can contribute to the cumbersome nature of an overly complex culture model. As such, a simple yet effective model for 3D culture is highly desirable. Finally, a 3D culture model must provide useful information. Towards this end, a highly representative environment is desirable. While scaffold can be made to mimic in vivo microenvironments, the extent to which this is possible is limited. Scaffolds tend to limit the amount of cell-cell connectivity possible. This is particularly important when considering models involving cells like cardiac myocytes that contain gap junctions that are essential to the functionality of said cells.

Many forms of 3D tissue culture have been evaluated up to this point (9). Microfluidics based systems enjoy the advantages of a potential control of the microenvironment of systems along with a potential for improved sterility. Unfortunately, complexity and cost limit microfluidics HTS models. Rotational bioreactors have the ability to spontaneously generate cell-dense 3D structures, however size and cost are limiting factors for HTS. Scaffold based systems also have the ability to generate 3D architecture, however they are limited by material type/complexity and ability to truly mimic *in vivo* conditions. A self-assembling model, requiring cells, one reagent and a few magnets provides a streamlined and simple model for the rapid generation of 3D organotypic tissues.

Cardiovascular drug development is one of the most important areas of pharmaceutical research with roughly 6 million people affected by heart disease in the United States (10). The large market combined with the difficulty of culture of cardiac myocytes in a 2D environment make a 3D cardiac tissue culture model highly desirable.

Culture of organotypic tissues is an area of much interest. *In vitro* tissue constructs with faithful representation of *in vivo* tissue characteristics are needed for screening and characteristic assessment of a variety of tissue types. Cardiac tissue analogs are particularly sought after due to the phenotypic degradation and difficulty of culture of primary cardiac myocytes. This study utilized magnetic nanoparticles and primary cardiac myocytes in order to levitate and culture 3D cardiac muscle-like tissue.

2. Materials and Methods

All animal protocols were approved by the Institutional Animal Care and Use Committee (IACUC) at the University of Houston. All materials were purchased from Sigma-Aldrich (St. Louis, MO) unless otherwise specified.

2.1. Isolation of primary cardiac cells

Cardiac cells were isolated from the hearts of 2–3 day old neonatal Sprague-Dawley rats using an established method (11). Tissues were minced into 1 mm^3 pieces and transferred to a dissociation solution (DS) consisting of filtered 0.32 mg/ml collagenase type 2 (Worthington Biochemical Corporation, Lakewood, NJ) and 0.6 mg/ml pancreatin in phosphate buffer. A 50 mL conical tube containing 15 mL of DS and the minced tissues was placed in an orbital shaker and maintained at 37 ℃ for 30 minutes at 60 rpm. At the end of the digestion process, the supernatant was collected in 3 ml of horse serum to neutralize the enzyme and centrifuged at 1,000 rpm for 5 minutes at 4 ℃. The cell pellet was re-suspended in 5 ml horse serum and kept in an incubator at 37 ℃ supplied with 5% CO_2. Fresh DS was added to the partially digested tissue and the digestion process was repeated an additional 2–3 times. Cells from all the digests were pooled, centrifuged and suspended in culture medium (CM) consisting of M199 (Life Technologies, Grand Island, NY), with 20% F12k (Life Technologies), 10% fetal bovine serum, 5% horse serum, 1% antibiotic-antimycotic, 40 ng/ml hydrocortisone and 100 ng/ml insulin. Cell concentration and viability was assessed by Trypan blue (4%) staining according to the manufacturer's protocol.

2.2. Magnetic levitation

Cells were converted to 3D cultures using the Bio-Assembler Kit (Nano3D Biosciences). (Figure 1) Two 50 mm tissue culture plate were coated with 3 ml of SYLGARD (PDMS, type 184 silicone elastomer) (Dow Chemical Corporation, Midland, MI). The plates were air dried for 2 weeks and sterilized with 80% ethanol before use. Cell containing CM was added to each petri dish and incubated at 37 ^oC for 30 minutes at 80 RPM with an MIO-based nanoparticle assembly (NanoShuttle; Nano3D Biosciences) at concentrations of 50 μL/10^6 cells or 33 μL/10^6 cells. Cell containing CM was subsequently centrifugued at 1000 rpm for 1 minute and the pellets were re-suspended to a concentration of 2.5 × 10^6 cells/mL CM. Nanoparticle treated cell suspensions were distributed in ultra lo-bind 24 well culture plates (Corning Inc., Tewksbury, MA) at desired concentrations with 400 μL of CM per well. Neodymium magnets with field strengths of 50G were immediately placed over each of the 24 wells of the culture plate to levitate the cells to the air-liquid interface.

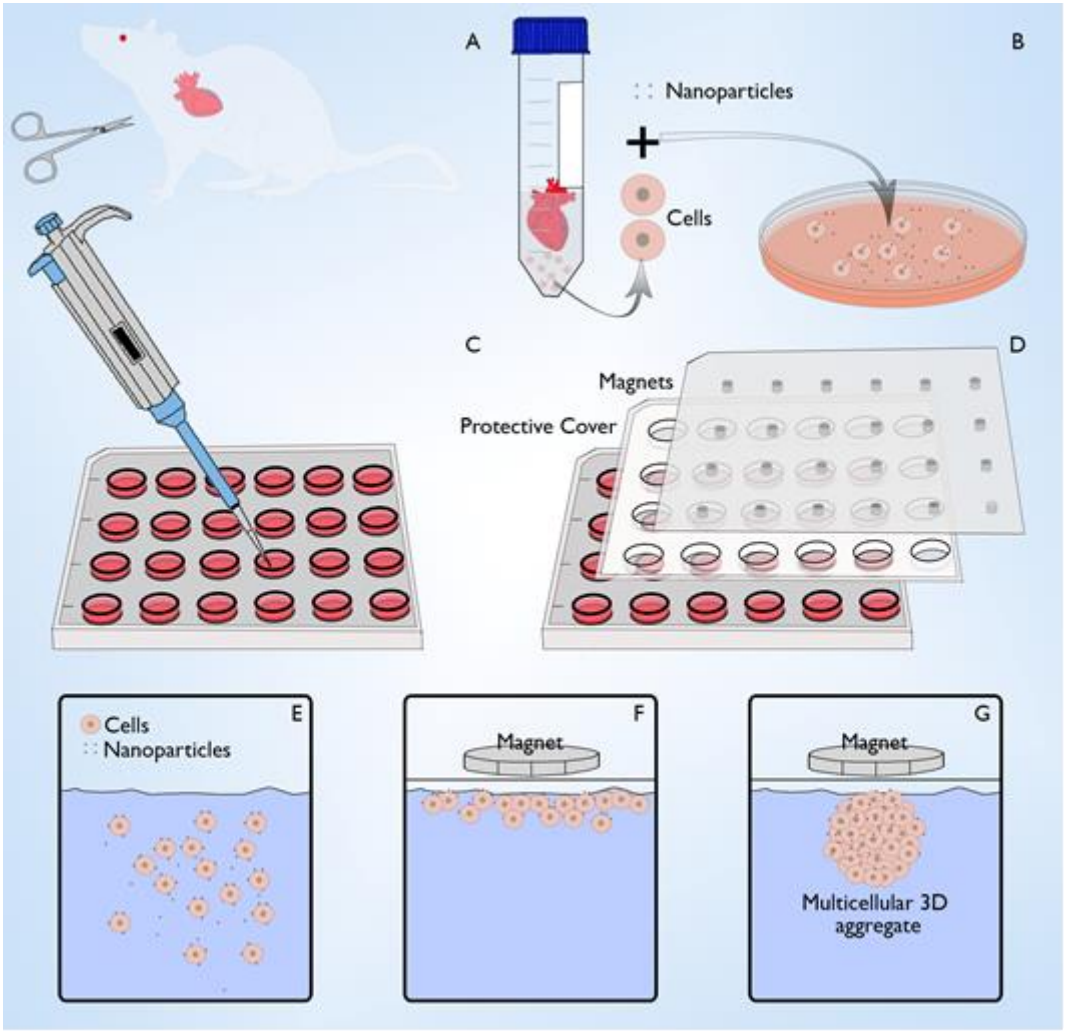

Figure 1. Schematic of magnetic levitation in a 24-well plate: Neonatal cardiac myocytes are isolated from 2–3 day old rats (A) and magnetically labeled with NanoShuttle (B, E). The magnetically labeled cells are distributed within the 24-well plate (C) in 400 μL of media and a magnet is applied to levitate the cells to the air-liquid interface (D, F). The levitated cells compact and form a cell dense MCA over time (G).

2.3. 3D culture formation and activity

Levitated 3D cultures were examined daily to examine contractile action and gross morphology using an inverted phase-contrast microscope (Nikon Instruments Inc., Melville, NY). Still photographs and videos were captured daily and examined using NIS elements software (Nikon Instruments Inc., Melville, NY), (Figure 2). Multicellular cardiac aggregates (MCAs) were picked up and placed as necessary during culture using a Teflon coated magnetic pen.

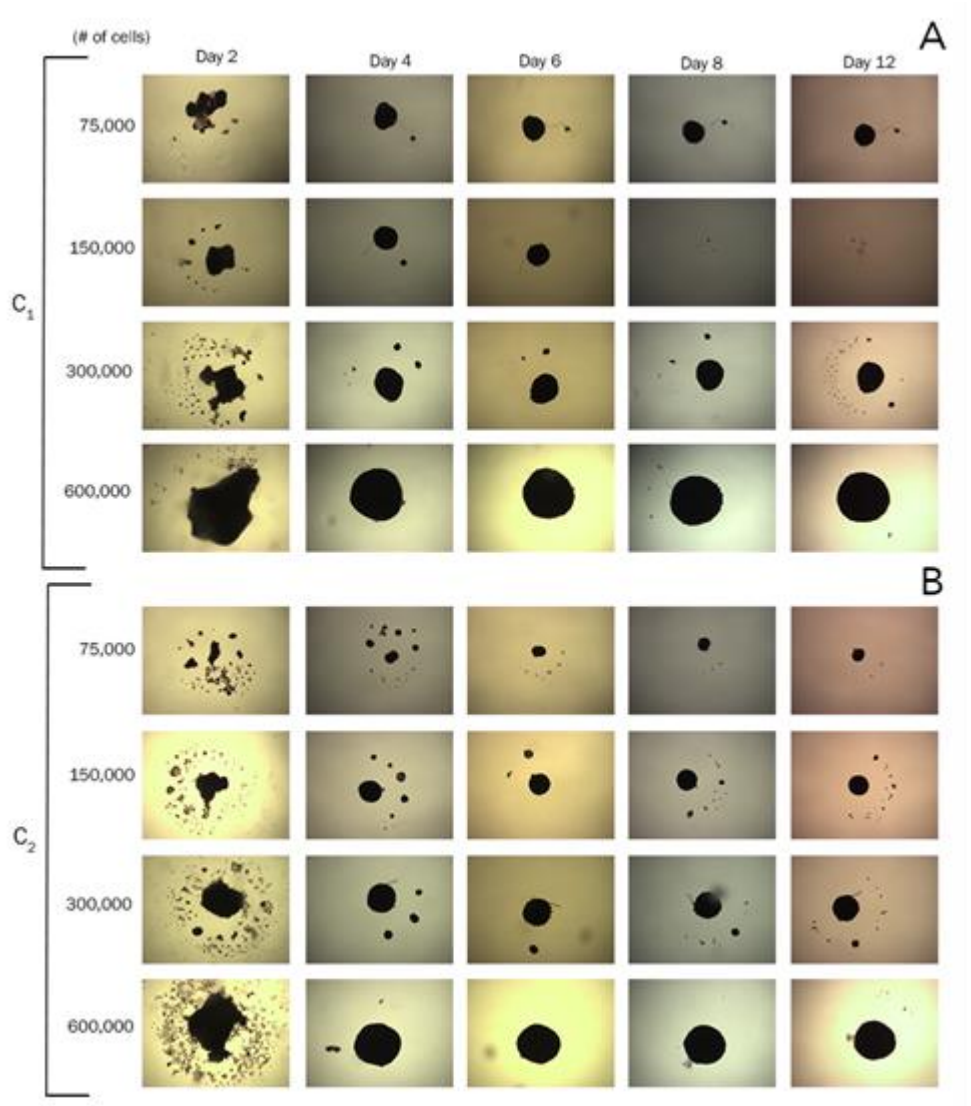

Figure 2. Bright-field images of MCA aggregate formations over time: Representative bright-field images are shown for each time point with varying initial concentrations of cells incubated with C1: 33 μLnanoshell/million cells (A) or C2: 50 μL nanoshell/million cells (B).

2.4. Histology and immunohistochemistry

For whole mount imunnohistochemistry (IHC), each sample was lifted from the 24 well culture plate and placed in a 96 well dish using a Teflon coated magnetic pen. A magnet was applied to the bottom surface of the 96 well dish to hold the samples in place. Samples were rinsed with PBS, fixed in 10% neutral buffered formalin (NBF) for 10 minutes, rinsed again, permeabilized with 0.5% Triton X-100 in PBS followed by a final wash. Cross-sections were obtained by freezing samples in OCT and sectioning them with a cryotome (Thermo Fisher Scientific, Waltham, MA). Cross-sections were fixed in ice-cold acetone for 10 minutes. Depth-specific cross-sections of entire particles were obtained at regular intervals for several samples. Nonspecific epitope antigens were blocked with 10% goat serum at room temperature for 1 hour for cross-sections and whole mount samples.

Samples were incubated with a combination of mouse anti-α-actinin monoclonal antibody (Sigma, Catalog No A7811), 1:200 with anti-cTnI (Abcam, ab47003), 1:200 with rabbit anti-collagen type I (Abcam, ab34710) 1:100, rabbit anti-CD31 (Abbiotec) 1:100 or rabbit anti-fibronectin (Abbiotec) 1:80 at room temperature for 1 hour. α-actinin presence was attributed to cardiac myocyte smooth muscle cells. CD31 was assessed in order to ascertain the localization and abundance of endothelial cells. Fibronectin was similarly observed for fibroblasts. (Figure 3)

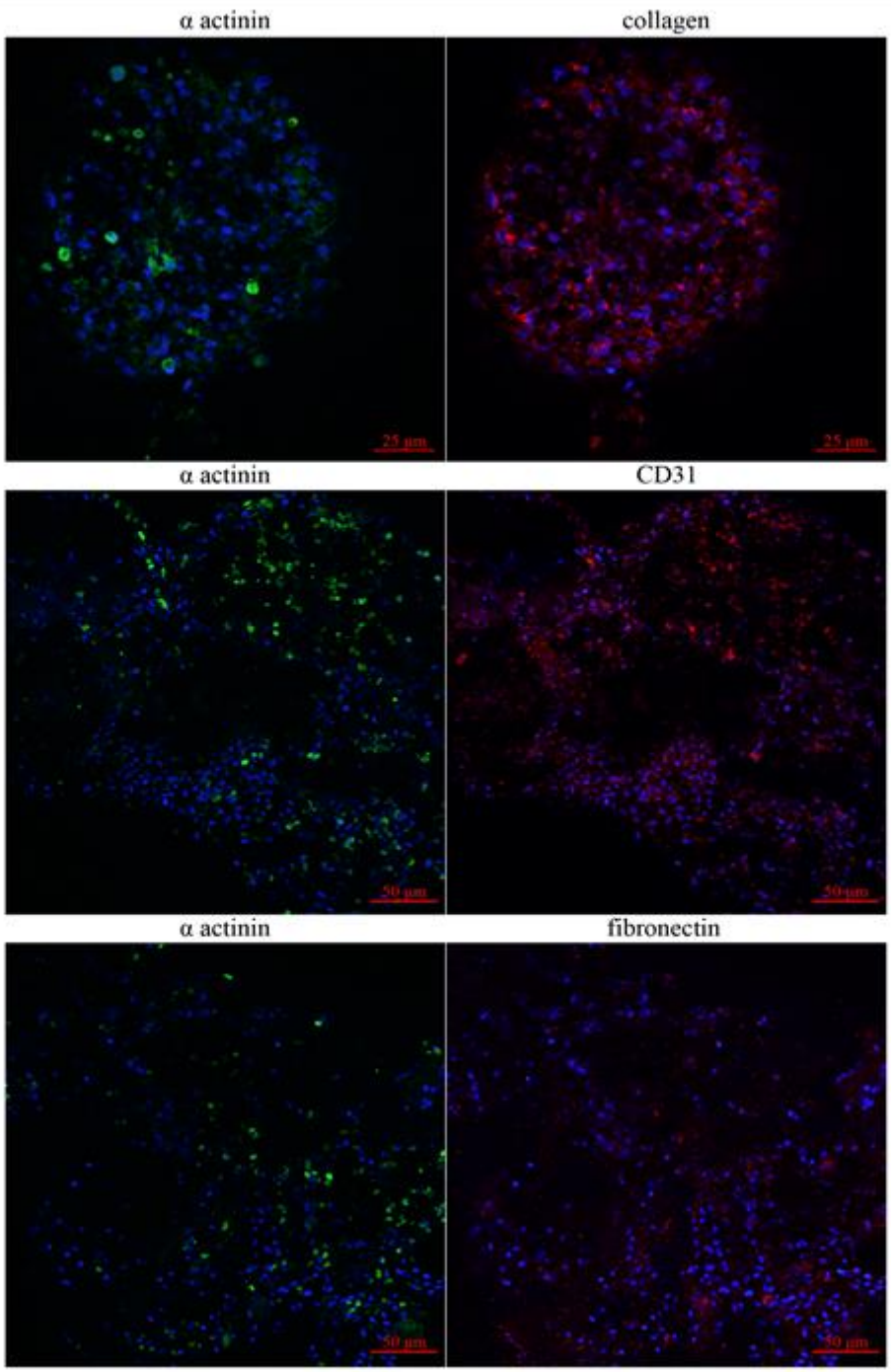

Figure 3. IHC images of whole-mount MCAs probed for α-actinin (green) and either collagen, CD31 or fibronectin (red).

Subsequently, samples were treated with goat anti-mouse and goat anti-rabbit secondary antibodies (Alexa Fluor 488 and Alexa Fluor 546, Life Technologies, Grand Island, NY) 1:400 at room temperature for 1 hour. Nuclei were counterstained with 4,6-diamidino-2-phenylindole (DAPI) (2.5 μg/ml) for 5 min at room temperature. Fluorescent images were obtained with a Nikon C2+ confocal laser-scanning microscope (Nikon Instruments Inc., Melville, NY). Z-stack images were taken in order to examine 3D structures of the samples. Masson's trichrome stains were performed on interval sections of an MCA and observed under a light microscope.

3. Results

3.1. Formation

Particles formed using the methods described above and illustrated in Figure 1 were reproducibly and readily produced. The process was repeated n = 10 times for a total of 240 MCAs formed with a variety of cell concentrations. Addition of the particles tended to cause clumping during the incubation phase; this means that isolated cells formed small aggregates during the initial 24 hours of the culture period. Simple agitation was sufficient to disrupt these transient interactions and re-disperse the cells in the medium. After application of the magnet, the cells moved to the air-liquid interface. By day 2, a centralized aggregate began to form. Within 4 days most cells were incorporated into the central aggregate with few remaining satellite structures. (Figure 2) There was little difference between the size and structure of 3D constructs generated using either C1 or C2 concentrations of nanoshell. Degradation of the constructs was witnessed at days 8 and 12, though this was less than 10%, based on the size of the aggregates. Constructs were generally stable in geometry and mostly remained intact through 12 days of culture. Satellite structures tended to merge with larger structures and compact slightly over time. MCAs were easily moved and manipulated using a Teflon-coated magnetic pen.

3.2. Activity

MCA contractions were observable beginning at day 3 or 4 and manifested in a variety of forms. Construct rotation, vibration and contortion were attributed to contractile action of the MCA. Contraction was clearly observable in 75 ± 8.8% (n = 24) of MCAs. Higher cell densities may correlate to a higher degree of observable contraction given that in one study MCAs with a density of 300,000 cells per well contracted observably 83.3 ± 10.8% (n = 12) of the time while those with a density of 100,000 cells per well contracted observably 66.7 ± 11.1% (n = 12) of the time. In the case of MCAs fabricated with higher cell densities (300,000 cells per MCAs), spontaneous contractions were noted for the 12-day duration of the culture. This was not the case for MCAs fabricated with lower cell densities (75,000 and 150,000 cells per MCAs); spontaneous contractions were noted earlier during the culture period and ceased after 6-8 days in culture.

3.3. Histology and immunohistochemistry

Immunohistological staining of whole-mount preparations confirmed a spherical architecture of the MCAs. (Figure 4) Three-dimensional images of MCAs probed for α-actinin and collagen illuminate the periphery of the spherical constructs. Interior portions were not visible in deeper z-slices of the stained preparations. Sections of an MCA at regular 100 μm intervals revealed cell-dense structures with pronounced collagen networks. (Figure 5)

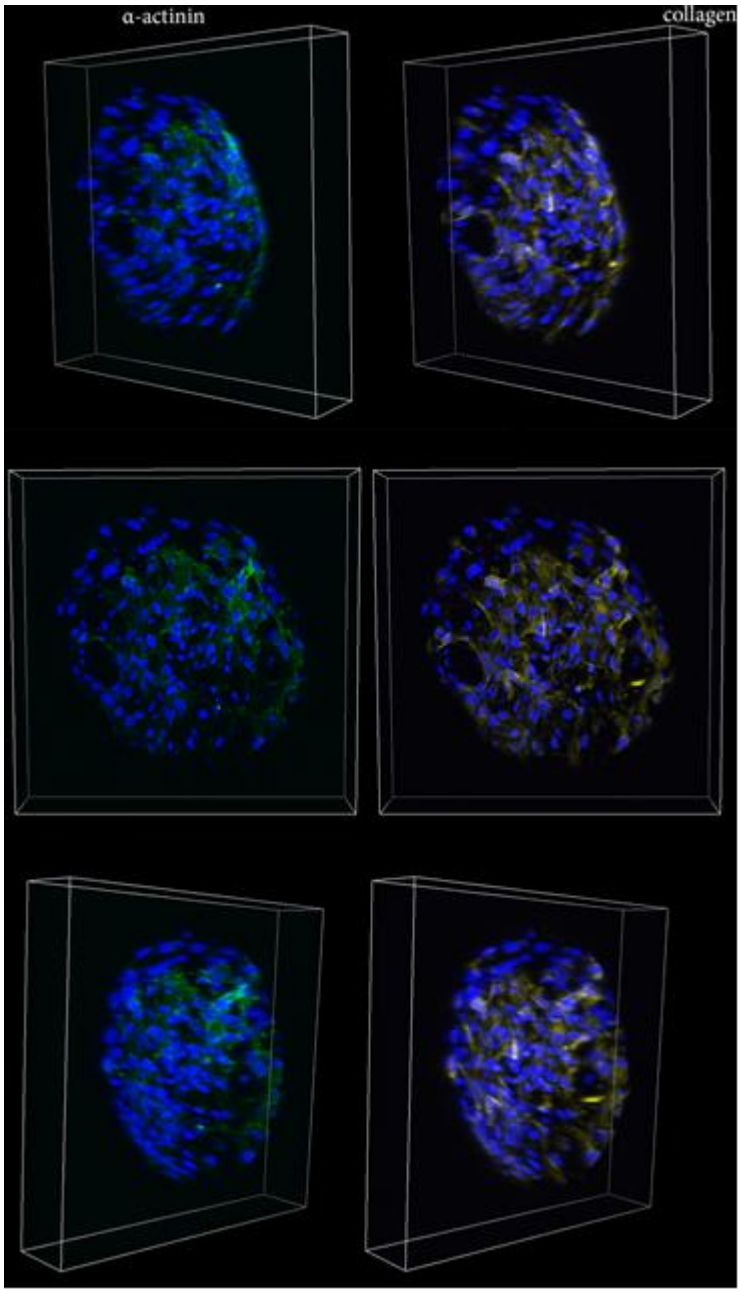

Figure 4. Z-stack 3D reconstruction of IHC images from whole-mount MCA: Sections are probed for α-actinin (green) and collagen (yellow). The z-stack reconstruction is displayed oriented to the left, middle, and right in order to display 3D

information and emphasize the spherical geometry of the MCA.

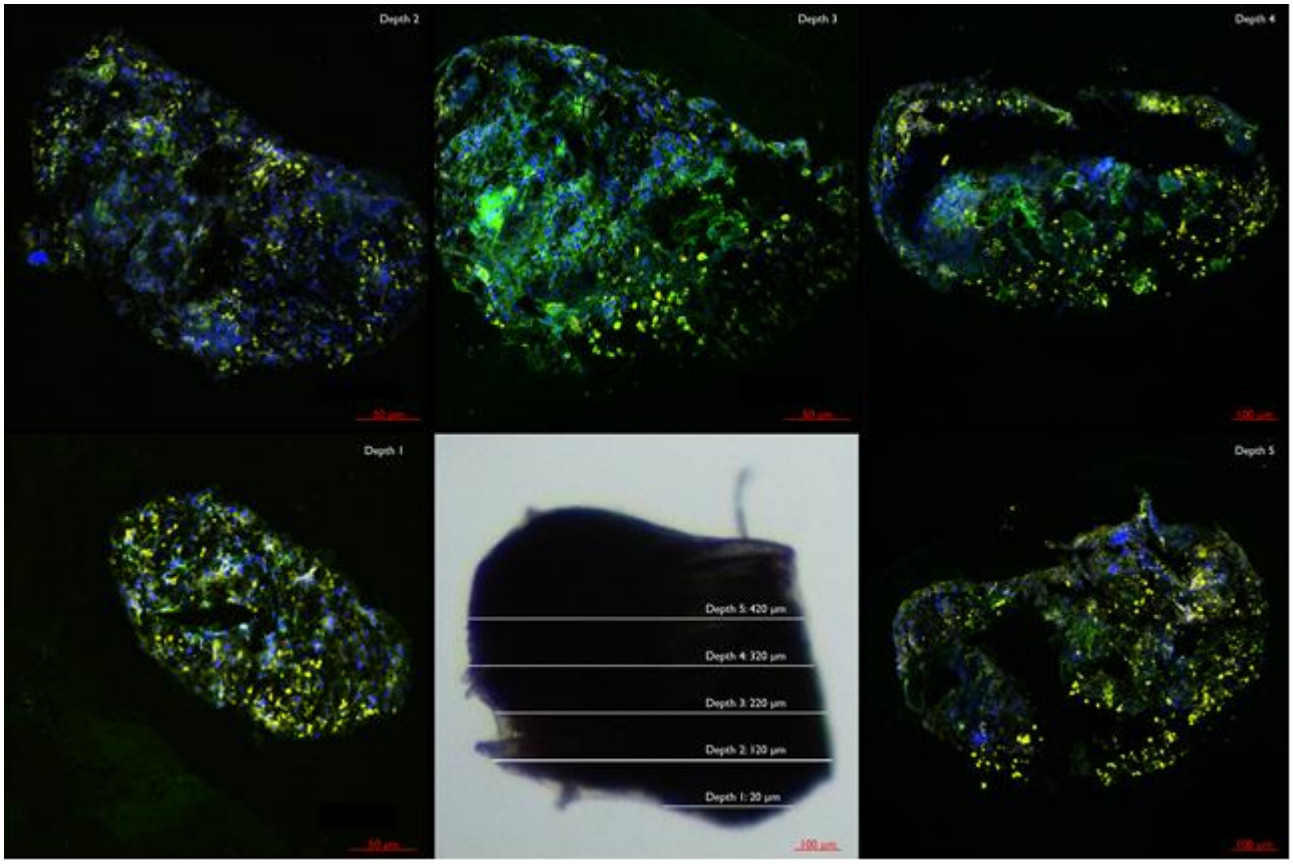

Figure 5. IHC images of sections of MCA at discrete depths: Sections are probed for α-actinin (green) and collagen (yellow) and the corresponding bright-field image of the MCA prior to sectioning. Section depth lines overlaying the bright-field image are not intended to describe exact geometries.

Interior portions were positive for α-actinin and DAPI stains confirmed cell-presence throughout. Z-band α-actinin formations can be seen, however alignment and fiber lengths are lower than in native tissues. (Figure 6B) MCAs probed for CD31 and Fibronectin illustrated protein presence under whole-mount preparations. MCAs probed for cTnI indicated troponin I presence along muscle fibers. (Figure 6A, B) Probes for ki67 illustrate that MCAs were positive for cellular division, and n-cadherin probes indicate moderate expression of the proteins at 12 days. (Figure 6. C, D)

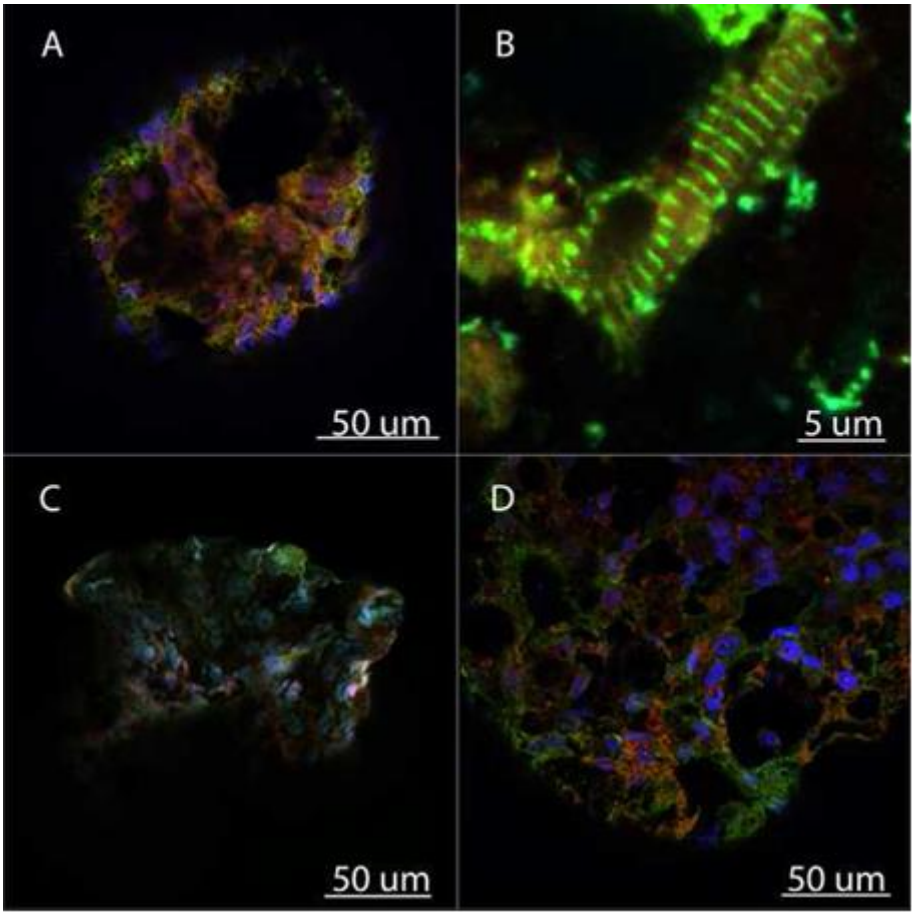

Figure 6. IHC images of whole mount MCAs: MCAs in all images were probed for α-actinin (green) and DAPI (blue). MCAs were secondarily probed for cardiac troponin 1 (red) in (A) and (B), ki67 in (C) and n-cadherin in (D). The image in (C) was taken at a higher magnification and shows distinct z-bands.

4. Discussion

The technique presented in this paper was used to successfully generate hundreds of MCAs with relative ease. The MCAs presented with similar geometry and formed with a 100% success rate. The ease with which this technique was applied to generate 3D cardiac structures using primary cardiac myocytes makes it an attractive multidimensional culture technique. MCA size manifested in approximate proportion to the number of cells used up to 600,000 cells, indicating a rough ability to control MCA size in culture. The amounts of nanoparticle added to the cells prior to levitation (C_1 and C_2) were proscribed based on results of preliminary studies. An estimated 1 μL per 10,000 cells had previously been used to successfully levitate other cell types, however it was quickly apparent that less particle could be used when incubating with the protocol described herein. Given that there was no discernable difference between C_1 and C_2 treated MCAs, it is conceivable that even less magnetic nanoparticle could be used, thus reducing the overall material cost. All studies were performed using a 24 well culture plate, however the technology could conceivably be scaled up to a 96 well system in order to increase throughput.

Most MCAs were observed to contract visibly under the light microscope, however it was difficult to visibly ascertain contractile frequency due to the small size of the particles along with the inherent oscillations of a moving object suspended under a magnet. The visible contractility serves as an obvious indicator of cardiac myocyte presence and phenotypic stability. It was observed that MCAs formed with higher concentrations of cells contracted more often under a light microscope. It may be that higher concentrations of cells allow for greater cardiac myocyte coordination and action, however the inherent uncertainty of qualitative assessment prohibits any conclusive analysis. Smaller MCA contraction may be present in proportionately similar amounts to those of larger MCAs. Given that there are less cells generating contractile action in smaller MCAs, the overall stabilizing force of the magnet may overcome the net contractile action of the cardiac myocytes.

Whole mount confocal assessment of the MCAs revealed alpha actinin, collagen, CD31 and fibronectin presence. Three-dimensional images of whole mount sections revealed interconnected networks around the perimeter of the MCAs for α-actinin and collagen. Interior portions of the MCAs were not visible using this method due to light scattering. In order to confirm cellular presence and activity of interior portions, interval sections of an MCA were probed for collagen and α-actinin. Interior sections revealed cellular presence and were positive for both collagen and α-actinin throughout the interior of the MCAs. The presence of fibroblasts, endothelial cells and SM cardiac myocytes indicate a similarity of cellular composition of the MCAs to cardiac smooth muscle. Furthermore, given that the confocal analysis was performed after 12 days of culture, positive stains for CD31, fibronectin and α-actinin indicate a degree of phenotypic stability.

The current study was designed as a proof of concept pilot to demonstrate the feasibility of forming 3D cardiac tissue using a novel magnetic levitation study. Initial histological assessment provides preliminary evidence to suggest the formation of 3D tissue that replicates a partial subset of heart muscle phenotype. Rigorous optimization studies are required to bridge the gap between with mammalian heart muscle tissue. Furthermore, functional metrics will need to be measured and include the twitch force of contraction, electrical activity and changes in calcium transients.

MCAs generated using the methods described above clearly generated 3D cell dense aggregates. The inter-dimensional cell-cell activity conferred not only phenotypic stability, but also allowed for continued functionality of the active cell types in cardiac muscle. Given the ease with which MCAs were generated and the similarity to heart muscle, the described technology presents an intriguing potential for high-throughput screening of cardiac muscle analogs.

Acknowledgements

The authors would like to thank Mohamed A. Mohamed for his contribution in reviewing the content presented herein and Nano3D Biosciences, for their help with magnetic levitation. This study was funded, in part, by the National Institute of Health (NIH) R01 Grant (EB011516).

Conflict of Interests

The University of Texas M. D. Anderson Cancer Center (UTMDACC) and Rice University, along with their researchers, have filed patents on the technology and intellectual property reported

here. If licensing or commercialization occurs, the researchers are entitled to standard royalties. G.R.S has equity in Nano3D Biosciences, Inc. UTMDACC and Rice University manage the terms of these arrangements in accordance to their established institutional conflict-of-interest policies.

References

1. Ehler E, Jayasinghe SN. Cell electrospinning cardiac patches for tissue engineering the heart. Analyst. 2014;139(18):4449-52.
2. Haraguchi Y, Shimizu T, Matsuura K, Sekine H, Tanaka N, Tadakuma K, Yamato M, Kaneko M, Okano T. Cell sheet technology for cardiac tissue engineering. Methods MolBiol. 2014;1181:139-55.
3. Hirt MN, Hansen A, Eschenhagen T. Cardiac tissue engineering: state of the art. CircRes. 2014;114(2):354-67.
4. Macadangdang J, Lee HJ, Carson D, Jiao A, Fugate J, Pabon L, Regnier M, Murry C, Kim DH. Capillary force lithography for cardiac tissue engineering. JVisExp. 2014(88).
5. Matsuura K, Masuda S, Shimizu T. Cell sheet-based cardiac tissue engineering. AnatRec(Hoboken). 2014;297(1):65-72.
6. Rao C, Barratt H, Prodromakis T, Terracciano CM. Tissue engineering techniques in cardiac repair and disease modelling. CurrPharmDes. 2014;20(12):2048-56.
7. Sapir Y, Polyak B, Cohen S. Cardiac tissue engineering in magnetically actuated scaffolds. Nanotechnology. 2014;25(1):014009.
8. Williams C, Budina E, Stoppel WL, Sullivan KE, Emani S, Emani SM, Black LD, III. Cardiac Extracellular Matrix-Fibrin Hybrid Scaffolds with Tunable Properties for Cardiovascular Tissue Engineering. Acta Biomater. 2014.
9. Galvez-Monton C, Prat-Vidal C, Roura S, Soler-Botija C, Bayes-Genis A. Cardiac Tissue Engineering and the Bioartificial Heart. RevEspCardiol. 2013;66(5):391-9.
10. Roger VL, Go AS, Lloyd-Jones DM, Benjamin EJ, Berry JD, Borden WB, Bravata DM, Dai S, Ford ES, Fox CS, Fullerton HJ, Gillespie C, Hailpern SM, Heit JA, Howard VJ, Kissela BM, Kittner SJ, Lackland DT, Lichtman JH, Lisabeth LD, Makuc DM, Marcus GM, Marelli A, Matchar DB, Moy CS, Mozaffarian D, Mussolino ME, Nichol G, Paynter NP, Soliman EZ, Sorlie PD, Sotoodehnia N, Turan TN, Virani SS, Wong ND, Woo D, Turner MB. Heart disease and stroke statistics--2012 update: a report from the American Heart Association. Circulation. 2012;125(1):e2-e220.
11. Tao ZW, Mohamed M, Hogan M, Gutierrez L, Birla RK. Optimizing a spontaneously contracting heart tissue patch with rat neonatal cardiac cells on fibrin gel. JTissue Eng RegenMed. 2014.

AIMS Press